Aspects of Applied Biology 77, 2006
International advances in pesticide application 2006

Modelling airflow through 3d canopy structure of orchards

By A MELESE ENDALEW, M HERTOG, P VERBOVEN, K BAETENS, M A DELELE, H RAMON, B M NICOLAÏ

Faculty of Bioscience Engineering, BIOSYST – MeBioS, Katholieke Universiteit Leuven
Willem de Croylaan 42, B-3001 Leuven, Belgium

Summary

Because of high costs for pest control and of intensified concerns for environmental protection, the need for improvements in spray efficiency and for drift reduction are more critical than ever before. Inefficiencies in spray applications are related to a complex combination of factors, including environmental conditions, tree architecture, development stages as well as machine design, calibration and operation. Accurate prediction of airflow through a canopy is difficult due to the complexity in the structure of vegetation elements and the complex process of air momentum transport within the canopy. This further makes it difficult to analyse particle deposition on plant canopies and drift so as to optimize design and operation parameters to equipments. In this work a 3D orchard canopy structure is developed by means of a plant growth model, which considers the phenomenological plant growing behaviour and effects of temperature and pruning. The resulting canopy architecture is introduced into a CFD package in order to model the 3D airflow through the canopy. The real effects of the canopy on the airflow distribution are investigated. The simulations are used to identify simplified canopy models that can be used in drift prediction models, which are mainly based on porous media theory.

Key word: orchard canopy, canopy architecture, airflow

Introduction

Wind, atmospheric airflow, is an important environmental factor for scalar fluxes (heat, water vapour, carbon dioxide, etc.,) and movement of spores, pollen and particles within a plant canopy (Zeng and Takahashi, 2000). As a result the numerical prediction of the natural phenomena of wind blown particles on plant canopies has attracted the attention of researchers from a wide range of engineering and scientific backgrounds (Alhajraf, 2003). However, atmospheric airflow in canopy structures tends to be strongly complex three-dimensional, inhomogeneous and turbulent. This creates difficulties in accurate numerical simulation and modelling of the interaction between the injected spray particle, the atmospheric airflow and the target plant canopy. Consequently porous medium models have been adopted, in which the transport properties of interest are averaged over a small volume of the crop to remove flow detail associated with individual crop elements (Zhi et al., 1997). A comprehensive introduction to the spatial-averaging procedure for crop canopy flow was given by Raupach and Shaw (1982), who employed a leaf area density (LAD) to represent the crop

structure and treated each variable as a spatial average over the total volume. Whilst current methods of modelling the transport and deposition process are good on a large scale they leave much to be desired on the scale of the individual plant and its elements.

The characterization of biological and physical processes in canopy models is usually based on the description of the geometric structure as a continuous medium. This approximation enables the use of differential equations to describe mass and energy transfer between plants and their environment (Fournier and Andrieu, 1998). In recent years, approaches have been developed to describe the geometric structure of plants in 3D. Most of these models are developed mainly on L-systems or similar approaches, to simulate the 3D architecture of plants (e.g. Prusinkiewicz and Lindenmayer, 1990) but little has been done to link these 3D plant canopy models with CFD to study the interaction of plants with their environment.

This work is intended to apply numerical methods on airflow through orchard canopy structures by introducing a detailed 3D structure of the canopy without leaves (worst case scenario to predict drift) into CFD software. To accomplish this objective plant growth algorithms have been employed in order to describe the 3D geometric structure of the orchard canopies and computational fluid dynamics (CFD), CFX 5.7.1 is used to model airflow through the canopy.

Materials and Methods

3D architectural modelling of the Orchard canopy

Plants consist of a large number of individual elements, where the configuration of these elements follows relatively simple rules (e.g. the branching pattern within a genus is usually constant) (Muhar, 2001). This enables plant modelling algorithms to find ways for a formal mathematical description of the 'genetic construction plan' of a plant. Here the architecture of the tree is simulated using a combined discrete continuous simulation model. The model is using ODEs to describe time and temperature dependent continuous growth functions. At the same time discrete events are introduced to indicate when certain thresholds are reached. The basic unit of the model is an object representing a single branch describing its life cycle starting as a bud, growing (if the level of growth inhibitor allows for this) to its final length, meanwhile producing growth inhibiting hormone which is exported to its predecessors, finally generating a new active apical bud with a number of (dormant) side buds. With that the cycle starts over again for each of the newly generated buds.

This model assumes an endogenous growth control mechanism; production of a growth inhibiting hormone (*GIH* [moles]) by the apex that is transported down through the branch inhibiting the side buds. The *GIH* turnover in a growing bud is assumed to be related to the constant production rate of *GIH* and some export term from the growing bud to the lower branch. By the time the growing bud has reached its maximum length the constant hormone production term ceases to exist. For any of the lower branches *GIH* turnover is ruled by the balance between import from the upper branch or bud or successor and export to the lower branch or predecessor.

The transport rate of *GIH* is not assumed to depend on temperature. The hormone balance is thus affected by exogenous mechanisms; seasonal temperature changes and pruning activities both affecting hormone production rate, inducing a new burst of growth. Depending on the hormone levels and the threshold levels assigned to each of the buds, one or more of the lower (dormant) side buds might (or might not) start to grow. All side buds remain actively waiting for their time to come (if ever) to start to growth. By the use of random factors in the angle under which branches develop, the threshold values of individual buds etc., the shape of the final tree can be manipulated. The exact positions of the branches are calculated using straightforward trigonometric relationships.

Some of the input parameters used in this modelling, therefore, include, growth rate of a branch, growth time in years, maximum and minimum stem radius within the growth time, maximum and

minimum branch length, growth activation energy, auxine exchange between branches, critical level of auxine for growth initiation of a new bud, numbers of side-buds per node, average growth angle of a new branch with the parent branch etc. These parameters are used to generate the 3D coordinates of the starting and end points of branch centrelines. The solid tree is developed by creating conical bodies around these centrelines. The stem of a branch, represented by a cone is defined by its length, bottom and top radius. The radii vary depending on the age of the branch.

Flow domain and boundary conditions

A representative free space domain with 30m length, 4m width and 8m height is used (fig.1). Two leafless canopies are put in the domain on the bottom ground (no-slip wall boundary) 10m and 11.5m from the inlet. The two sides of the domain that extend 2m from the central xy plane are taken as symmetry planes. Above the immediate influence of the obstacles, the flow in the Atmospheric Boundary Layer (ABL) becomes more homogeneous (Macdonald, 2000). The mean velocity in this sub-layer is described by the classical logarithmic profile. Based on the assumption that the log law holds all the way down to the top of the obstacles (Ayotte et al., 1999), a developed logarithmic velocity profile is imposed at the inlet (fig.1), which is the simplest consistent assumption we can make about conditions on the soil surface below the canopy. Constant gradients are assumed for turbulence kinetic energy k and its eddy dissipation rate ε is a function of height y and the friction velocity u_* within the ABL. The outlet and the top of the domain are made pressure and Cartesian velocity outlet boundaries respectively.

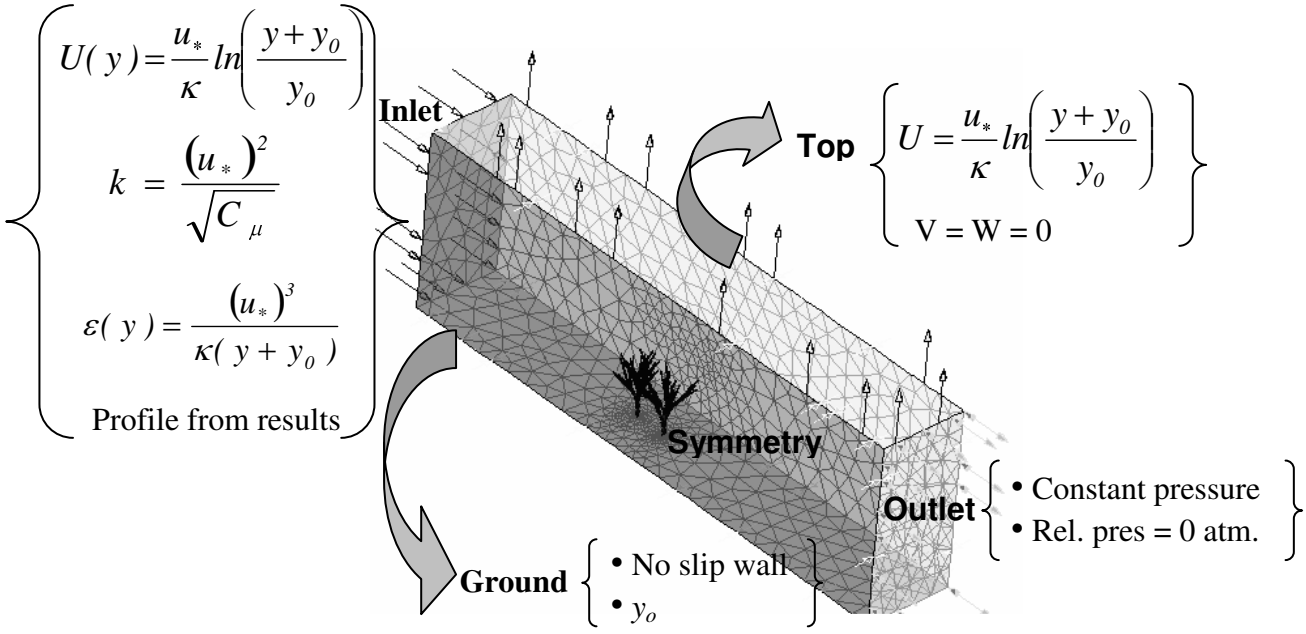

Figure 1: Initial and boundary settings

Airflow model governing equations

Sanz (2003) on his note on 'k-ε modelling of vegetation canopy air-flows' mentioned that the k-ε turbulence model is a standard of computational software packages for engineering, yet its application to canopy turbulence has not received comparable attention. This is probably due to the additional source (and/or sink) terms, whose parameterization remained uncertain. The two equation *k*-ε model is the most popular in engineering application and is used in several spray

models (e.g. Brown and Sidhamed, 2001). The k-ε turbulent equations supplemented by additional source terms were used to model airflow within and above vegetation canopies using porous media approaches, which applies spatial averaging assumptions. An important advantage of this assumption is the possibility to use a commercial CFD solver for the resulting equations (Da Silva et al., 2005). However, in this work, since 3D canopy structure is introduced into the domain, *k-ε* model is used without source or sink term. The CFD code used for this modelling is CFX 5.7.1 (ANSYS, Inc., Canonsburg, Pennsylvania, USA). The set of equations solved by CFX-5 are the Reynolds-averaged Navier-Stokes (RANS) equations in their conservation form. The three-dimensional spatio-temporal RANS equations of mass and momentum conservation for an incompressible, viscous, isothermal flow of a Newtonian fluid, in Cartesian co-ordinates, in partial differential equation form and in conservation form are given as follows:

$$\frac{\partial(\rho u_i)}{\partial x_i} = 0 \tag{1}$$

$$\frac{\partial \rho u_i u_j}{\partial x_j} = -\frac{\partial p}{\partial x_i} + \frac{\partial}{\partial x_j}\mu\left(\frac{\partial u_i}{\partial x_j} + \frac{\partial u_j}{\partial x_i}\right) - \frac{\partial}{\partial x_j}(\rho \underbrace{\overline{u_i' u_j'}}_{=R_{ij}}) \tag{2}$$

Where u_i is the i^{th} component of the averaged velocity [m/s], t is the time [s], p is the average pressure [Pa], ρ is the density of the fluid which is assumed constant [kg/m³], x_i ($i=1,2,3$) is the Cartesian coordinate, μ is the dynamic viscosity [kg/ms], u_i' and u_j' are fluctuating velocity parts [m/s]. In the *k-ε* model the turbulent Reynolds stress tensor, R_{ij} in eq. (2) is modelled by adopting the extended Boussinesq hypothesis (Versteeg and Malalasekera 1995), which relates the turbulent stresses to the mean rate of deformation:

$$R_{ij} = -\frac{\mu_t}{\rho}\left(\frac{\partial u_i}{\partial x_j} + \frac{\partial u_j}{\partial x_i}\right) + \frac{2}{3}k\delta_{ij} \tag{3}$$

where μ_t is the turbulent viscosity [kg/ms], k is turbulent kinetic energy [m²/s²] and δ_{ij} is the Kronecker delta ($\delta_{ij} = 1$ if $i = j$ and $\delta_{ij} = o$ if $i \neq j$). μ_t in *k-ε* model can be related with *k* and turbulent kinetic energy dissipation rate, ε [m²/s³]:

$$\mu_t = \frac{\rho C_\mu k^2}{\varepsilon} \tag{4}$$

The turbulent modifications are production of turbulent kinetic energy (from the mean kinetic energy of the airflow) and the dissipation of the wakes by the elements of vegetation. The representation of the turbulence is an important point of discussion (e.g. Wilson and Shaw, 1977; Katul et al., 2004; Finnigan, 2000). *k* and ε are modelled from the standard *k-ε* model:

$$\frac{\partial \rho k u_j}{\partial x_j} = \frac{\partial}{\partial x_j}\left(\frac{\mu_t}{\sigma_k}\frac{\partial k}{\partial x_j}\right) + P_k + \rho\varepsilon \tag{5}$$

$$\frac{\partial \rho \varepsilon u_j}{\partial x_j} = \frac{\partial}{\partial x_j}\left(\frac{\mu_t}{\sigma_\varepsilon}\frac{\partial \varepsilon}{\partial x_j}\right) + C_{1\varepsilon}\frac{\varepsilon}{k}P_k - \rho C_{2\varepsilon}\frac{\varepsilon^2}{k} \tag{6}$$

The production of kinetic energy in these equations is given by:

$$P_k = \mu_t\left(\frac{\partial u_i}{\partial x_j} + \frac{\partial u_j}{\partial x_i}\right)\frac{\partial u_i}{\partial x_j} \tag{7}$$

The conventional model constants are $C_\mu = 0.09$, $C_{1\varepsilon} = 1.44$, $C_{2\varepsilon} = 1.92$, $\sigma_k = 1.0$, and $\sigma_\varepsilon = 1.3$.

Mesh generation and solution procedure

An unstructured control volume mesh is used to discretise the computational fluid domain. For the meshing a maximum edge length of 1 m is defined for the free space with a minimum size of 1 mm on the surface of the smallest canopy branch which reduces to the maximum edge length for 8 layers. This mesh consists of 2841603 tetrahedral elements uniformly distributed over the domain with a total number of 526383 nodes. The solution converged to a normalized RMS residual of less than 10^{-7} of all equations after 500 iterations. Total CPU time of calculation was about 42 hours on an Intel Pentium IV, 2.8GHz Win2002 workstation with 1 GB of RAM computer. Placement of the trees on the ground and mesh refinements are shown in fig.2.

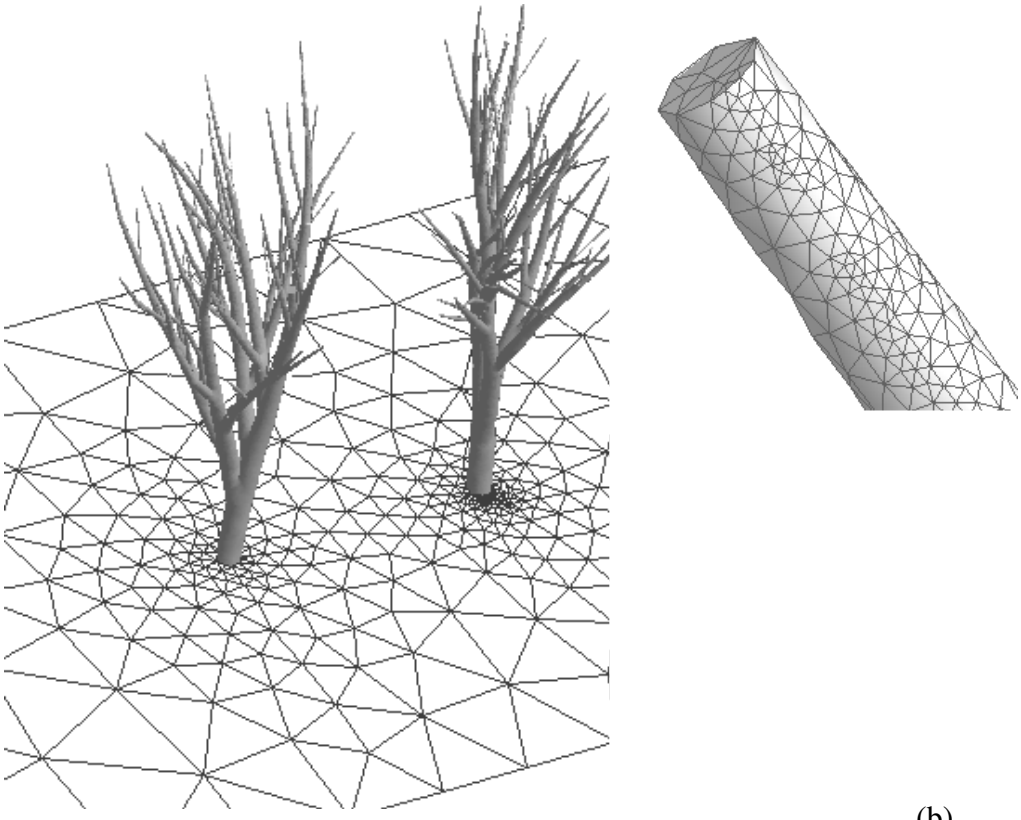

(a) (b)

Figure 2: The trees on the ground surface showing mesh refinement near the tree on the ground (a) and mesh on the surface of the smallest branch (b)

Results

The first simulations were done with two trees 1.5m apart in the domain (fig.1) and results of normalized longitudinal velocity *U* profiles taken before, after and between the canopies are shown in fig.3. *U* is normalized with the friction velocity u_* in the ABL and domain height Y is normalized with the height of the tree *h*. The velocity profiles captured in this simulation have been compared and are inline with the results obtained by Gross (1987) on his work on numerical study of the air flow within and around a single tree. In the second simulations the flow has been recycled in the domain using the output of the preceding run as an input for the proceeding one to see what happens to the flow in the inner part of the orchard field assuming that the field is symmetric along the rows. For this simulation the two trees were placed 1.5m and 3m from the inlet whereby the flow is assumed as if it was taking place in a continuous long field. The results are shown in fig.4 and compared with a wind profile with in canopy surface.

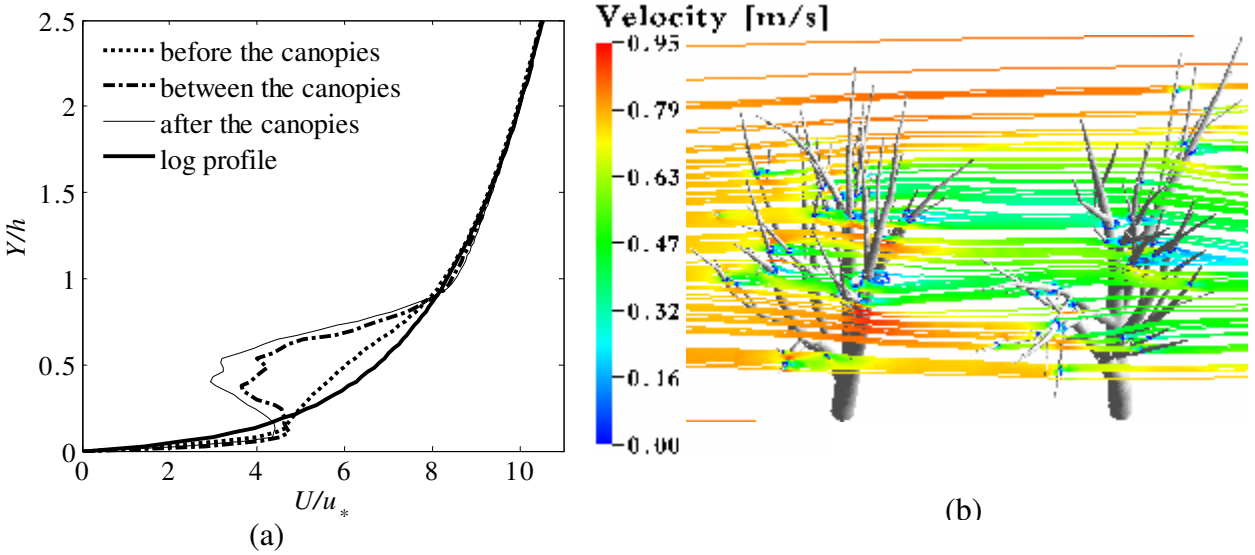

Figure 3: Normalized average vertical profiles of longitudinal velocity (a) and velocity streamlines (b) obtained from the first simulation at h = 1.75m

Discussion

The determination of the typical patterns of physical quantities within vegetation canopies is difficult because of the complex airflow dynamics determined by the spatial variability of the canopy elements. However the general notion is that there is an overall reduction of air velocity through the canopy due to flow resistance by the canopy elements. Fig.3 (a) shows this reduction of the average longitudinal air velocity where the extent of reduction depends on canopy density. In the figure it is shown that the reduction is higher at about half the height of the tree where the density is relatively high and it decreases on the upper and lower parts.

In the studies made so far on airflow within and above vegetation and forest canopies (Gross, 1987; Jacobs et al., 1995; Georgiadis et al., 1996; Zeng et al., 2000; Albertson et al., 2001; Turnipspeed et al., 2003) most of the results showed that the vertical velocity profiles show three characteristic regions, namely the canopy flow region, the transition flow region and the logarithmic region. The first canopy flow region is the region where the flow is highly dominated by the canopy density and architecture. It is characterized by a turbulence structure strongly affected by the large roughness elements of the tree. It is considered to be driven by the stress applied at the

canopy top by the outer velocity (Da Silva et al., 2005). The distribution of velocity in the canopy layer then depends on the turbulence structure within the region and the boundary conditions, continuity at the interface, and no-slip at the ground level. It covers the region from the ground to the canopy height *h*. In the second transition flow region just above the canopy, the vertical profiles significantly differ from the upper logarithmic layer and the inner canopy sublayers due to the fact that the turbulent transport is strictly related to the underlying canopy architecture. The depth of the region is strongly dependent on the canopy height and density variability (Georgiadis et al., 1996). The last logarithmic flow region is the region where the wind speed under neutral atmospheric conditions is described by the classical logarithmic profile. As it is shown in fig.4 (a), the results of this work showed these three characteristic regions clearly.

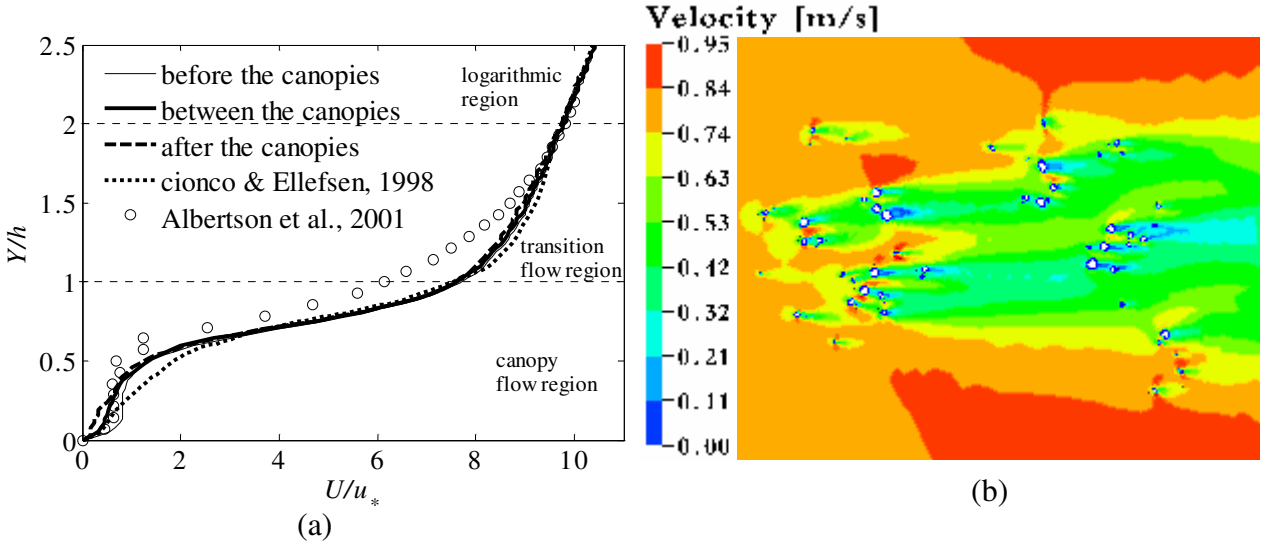

Figure 4: Normalized average vertical profiles of *U* obtained from the cyclic simulation representing wind profile in orchard field (a) and velocity contour at h = 1.75m (b)

Previously it was impractical to account explicitly for the spatial variability imposed on the airflow by the complexity of the within-canopy air space. In reality the interaction of the wind field within the foliage produces large amounts of fine-scale velocity reduction in the wakes of canopy elements. It was hardly possible to show these fine-scale reductions in the previous methods. With this method it has been possible to show them as shown by velocity streamlines in fig.3 (b) and contour plot in fig.4 (b). All simulations show an overall reduction of wind speed inside the tree, an accelerated flow over the tree and around the branches and a wake region in the lee.

Georgiadis et al., (1996) found that comparing the influence of the varying meteorological conditions and canopy characteristics on the airflow, the geometry of the obstacle is the dominant factor. The numerical approach presented here considers the real local effects of vegetation elements to airflow by introducing canopy architecture into a simulation domain. The simulation results obtained by this approach agree qualitatively with available wind tunnel measurements and previous works in the area. Although it needs to be validated, the approach may potentially resolve some of the problems attributed to porous media approaches to model air and particle flow through orchard canopies and the resulting drift.

Acknowledgements

The Flemish and Belgium governments are gratefully acknowledged for financial support (S-6209 and IWT-20424). Pieter Verboven is postdoctoral researcher for the Fund for Scientific Research – Flanders (FWO–Vlaandern).

References

Albertson J D, Katul G G and Wiberg P. 2001. Relative importance of local and regional controls on coupled water, carbon, and energy fluxes. Advances in Water Resources 24, pp 1103- 1118.

Alhajraf S. 2004. Computational fluid dynamic modeling of drifting particles at porous fences. Environmental Modelling & Software 19, pp 163-170.

Ayotte K W, Finnigan J J and Raupach M R. 1999. A Second-Order Closure for Neutrally Stratified Vegetative Canopy Flows. Boundary-Layer Meteorology 90, pp 189-216.

Brown R B and Sidhamed M M. 2001. Simulation of spray dispersal and deposition from a forest airblast sprayer- Part III: droplet trajectory model. Transactions of the ASAE 44(1), pp 11-24.

Cionco R M. and Ellefsen R. 1998. High resolution urban morphology data for urban wind flow modelling**.** Atmospheric Environment 32, pp7-17.

Da Silva A, Sinfort C, Tinet C, Pierrat D and Huberson S. 2005. A Lagrangian model for spray behaviour within vine canopies. Journal of Aerosol Science, In Press.

Finnigan J. 2000. Turbulence in plant canopies. Annual Review of Fluid Mechanics 32, pp 519-571.

Fournier C and Andrieu B. 1998. A 3D Architectural and Process-based Model of Maize Development Annals of Botany 81, pp 233-250.

Georgiadis T, Dalpane E, Rossi F and Nerozzi F. 1996. Orchard-atmosphere physical exchanges: modelling the canopy aerodynamics. Acta Hort. 416, pp 177-182.

Gross G. 1987. Numerical study of the air flow within and around a single tree. Boundary-Layer Meteorology 40, pp 311–327.

Jacobs A F G, van Boxel J H and El-Kilani R M M. 1995. Vertical and horizontal distribution of wind speed and air temperature in a dense vegetation canopy. Journal of Hydrology 166, pp 313-326.

Katul G G, Mahrt L, Poggi D and Sanz C. 2004. One- and Two-Equation Models for Canopy Turbulence. Boundary-Layer Meteorology 113, pp 81–109.

Macdonald R W. 2000. Modelling the Mean Velocity Profile in the Urban Canopy Layer. Boundary-Layer Meteorology 97, pp25–45.

Muhar A. 2001. Three-dimensional modelling and visualisation of vegetation for landscape simulation. Landscape and Urban Planning 54, pp 5-17.

Prusinkiewicz P and Lindenmayer A. 1990. *The algorithmic beauty of plants.* New York, Springer-Verlag.

Raupach M R and Shaw R H.1982. Averaging procedures for flow within vegetation canopies. Boundary-layer meteorology 22, pp 79–90.

Sanz C. 2003. A Note on *k* Modelling of Vegetation Canopy Air-Flows. Boundary-Layer Meteorology 108, pp 191 –197.

Turnipspeed A A, Dean E A, Peter D B, William M B and Russell K M. 2003. Airflows and turbulent flux measurements in mountainous terrain: Part 1. Canopy and local effects. Agricultural and Forest Meteorology 119, pp 1-21.

Versteeg H K & Malalasekera W. 1995. An introduction to computational fluid dynamics. The finite volume method. Englewood Cliffs, NJ: Prentice-Hall, 257 pp.

Wilson N R and Shaw R H. 1977. A higher order closure model for canopy flow. Journal of Applied Meteorology 16, pp 1197–1205.

Zeng P and Takahashi H. 2000. A first-order closure model for the wind flow within and above vegetation canopies. Agricultural and Forest Meteorology, 103, pp 301-313.

Xu Z G, Walklate P J and McLeod A R. 1997. Numerical study of a full-size free-air fumigation system. Agricultural and Forest Meteorology 85, pp 159-170.